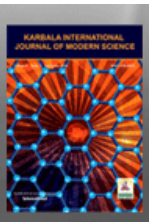

Karbala International Journal of Modern Science

Volume 6 | Issue 2 Article 12

On The Dynamic Behaviour of Automobile Pulleys Under Cyclic Loading

Haval Kamal Asker
University of Duhok, haval.k.asker@gmail.com

Thaker Saleh Dawood
University of Duhok, thaker.saleh@uod.ac

On The Dynamic Behaviour of Automobile Pulleys Under Cyclic Loading

Abstract

This paper investigates the dynamic characteristics of pulley systems with different numbers of bolt holes. Models with four, six and eight bolt holes were chosen for the pulley. Three sets of cyclic pressure were applied to the pulley system to resemble the different running revolutions of an engine. The study investigates the effect of the number of holes on the system's stiffness and natural frequency. Finite element models were used to simulate the obtained deformations, stresses and frequency response function (FRF) for pulley models comprising four, six and eight bolt holes under different cyclic pressures. The results show that the stiffness and natural frequency increased with increasing the number of the bolt holes. This in turn, reduced the resulted deformations and stresses.

Keywords

Keywords; Pulley, dynamic, vibration, holes, belt, natural frequency

1. Introduction

The design of the pulley in terms of parameters such as natural frequency, stiffness and maximum deformations and stresses plays an essential role in specifying the pulley's dynamic characteristics. Most researches on pulley design have focused on the effects of pulley rim thickness, dimensions of the pulley, manufacturing material and type of loading. These researches have mainly been performed at static condition. Finite element modeling plays important role in predicting dynamic behavior of complex structures in automobile industry.

Uddanwadiker [1] investigated the design of arm thickness of a pulley at different angular placements and the effect of the bending moment on the pulley arms. The study proposed the use of the radius to the rim thickness to determine the share of the bending moment. The use of different materials in manufacturing pulleys was studied by Veenitha et al. [2], Singathia and Aggarwal [3], and Madhavi et al. [4]. Veenitha et al. [2] employed finite element models to simulate the use of different materials at static loadings. They suggested using ANSYS software to facilitate the simulation of experimental works. ANSYS software was applied in the work of Singathia and Aggarwal [3] to study the deformations and stresses obtained by using different materials. The study reported that the main reason for failure of the pulleys was connected with the material selected. However, based on the small differences in the compared results, the authors indicated that the design of the pulley could play a more important role in identifying failure reasons. Additionally, Madhavi et al. [4] used CATIA and ANSYS software to model and analyze motor pulleys made of different materials. Based on the results of study, cast iron is a better material when compared to other materials such as aluminum and steel. The study used a coefficient of friction of 0.12 in their work, but concluded that this coefficient does not reflect the reality situation. They attributed this to the contact being steel-belt contact and not steel−steel contact.

Kim et al. [5] and Junhui and Yuan [6] built finite element models of a pulley loaded at its half diameter. Kim et al. investigated the history of the load during pulley rotation, at step 10°, using simulation. It suggested that a modified design for the bolt hole surface, but the centrifugal force was neglected in their work. Junhui and Yuan, loaded and analyzed a pulley of a crane. Their study involved merely static analysis of the pulley, with the pulley given specific dimensions.

It is apparent that most of the previous research neglected the dynamic behavior of the pulley and focused on static analysis. Also, the effect of the centrifugal force was ignored in most cases. The current paper sheds light on the effect of pulley design on the dynamic characteristics, taking into account to consider the centrifugal force effect. Three different models of pulley were proposed in this study: pulleys with four bolt holes, six bolt holes and eight bolt holes. Natural frequencies and frequency response functions (FRF) were obtained for the three pulley models.

2. The model

This study investigates the effect of number of bolt holes in the frame of the pulley on the dynamic characteristics such as natural frequency and transient response of the pulley system to cyclic loading. For this purpose, models with four, six and eight bolt holes were selected. The dimensions of the pulley are shown in Table 1. The model was adopted from a car engine pulley. Fig. 1 shows different views of the pulley model.

3. Load assumption

Estimation of the pressure applied to the pulley during loading is required in order to determine the amount of the cyclic loading presented in Section 6. As explained in this section, the pressure is calculated through the use of belt-pulley theories as shown in Fig. 2. It is necessary to determine characteristics such as the mass of the belt m, the velocity V, the tension of the belt at the tension side T_1, the tension of the belt at the slack side T_2, and the angle of contact θ.

For this research work, the rotation of the pulley N is assumed to be 2000 rpm, 3000 rpm and 4000 rpm, values approximating to the normal running rotation speeds of the engine [7,8]. In order to find the linear velocity (m/s) [9]:

$$V = r\,.\,\omega = \frac{r2\pi N}{60} \tag{1}$$

where ω is the angular velocity (rad/sec), r is the radius of the pulley and N is the revolutions per minute of the pulley. The linear velocities are 17.79 m/s, 26.69 m/s

https://doi.org/10.33640/2405-609X.1603

Table 1
Dimensions of the pulley.

S/No.	Parameters	Value	Unit
1	Radius	85	mm
2	Thickness	5	mm
3	Height	45	mm
4	Belt's length	1500	mm
5	Coefficient of friction (μ)	0.25	
6	Density (ρ)	1522	kg/m3
7	Revolution (ω)	3000	rpm

and 35.58 m/s respectively, obtained from pulley rotations of 2000 rpm, 3000 rpm and 4000 rpm.

The mass per unit length is measured by specifying the density of the belt and cross section dimensions. The density of the rubber belt (ρ) is 1522 kg/m^3 [10]. The width (b) and the thickness of the belt (t) are 45 mm and 5 mm respectively.

$$m = \rho.b.t \tag{2}$$

$$m = 0.3425\, kg/L \tag{3}$$

Using the equation below [9], the maximum tension in the belt can be calculated as follows:

$$V = \sqrt{\frac{T}{3m}} \tag{4}$$

where V (m/s) is the linear velocity, T (N) is the maximum tension in the belt and m (kg) is the mass per unit length. The length of the belt L is assumed to be 1500 mm.

$$T = 3(m/L).L.V^2 \tag{5}$$

Now, the maximum tension in the belt can be considered as the tension in the tension side of the belt T_1. In order to find the tension in the slack side of the belt T_2, the equation below can be utilized [9]:

$$\frac{T_1}{T_2} = e^{\mu.\theta} \tag{6}$$

where μ is the coefficient of friction between the belt and the pulley and θ (rad) is the angle of contact:

$$\theta = (180^\circ - 2\alpha)\,\frac{\pi}{180^\circ} \tag{7}$$

α is the angle between the point where the belt disconnects with the pulley and the vertical axis of the pulley. In this paper, α is equal to zero. Therefore $\theta = \pi$

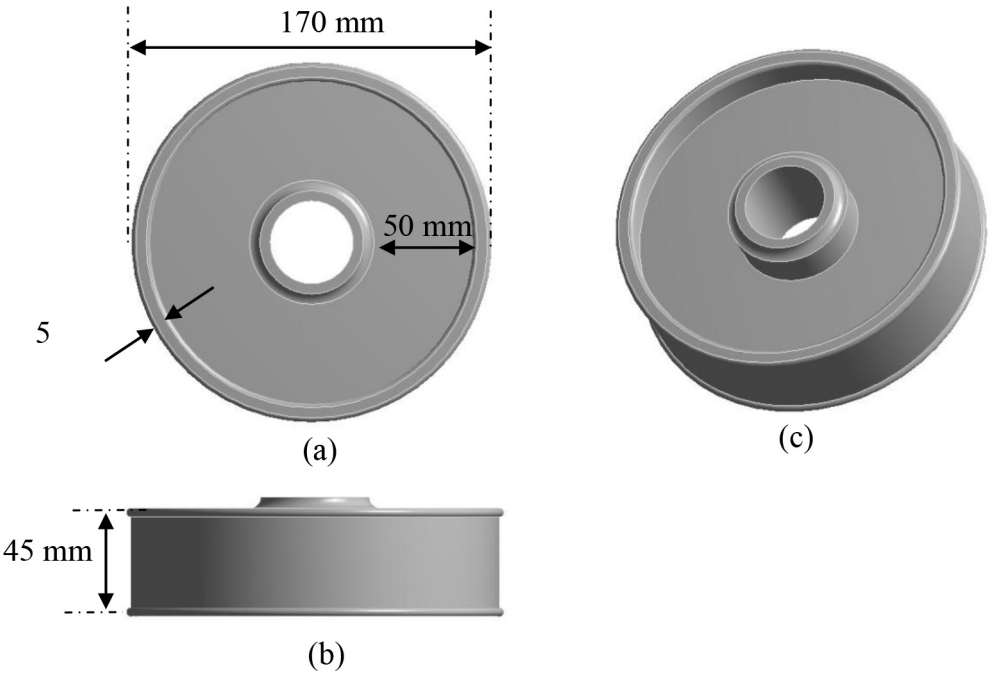

Fig. 1. Depicting the pulley model from its (a) top view (b) side view and (c) isometric view.

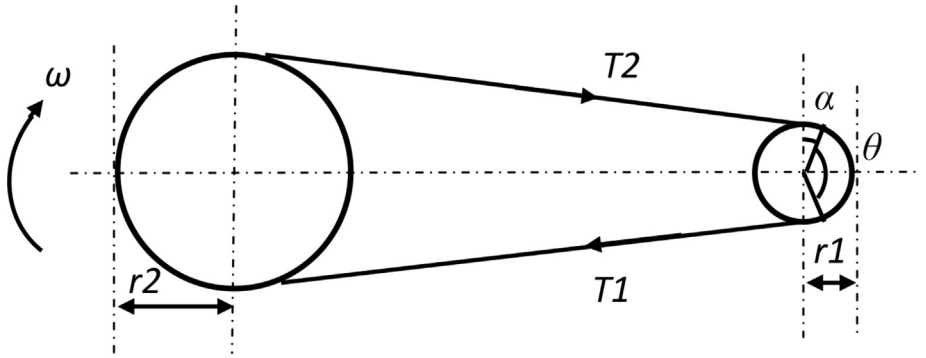

Fig. 2. Belt-pulley system.

rad. When α is set to zero, this means that the two pulleys are connected by the belt have the same diameter. The coefficient of friction is assumed to be 0.25 [11].

As the belt rotates around the pulleys in a continuous state, a centrifugal force will consequently be generated in the belt. The generation of the centrifugal force depends on the speed of the pulley. For speeds less than 10 m/s, the centrifugal force can be ignored, but if the speed is more than 10 m/s the centrifugal tension should be added to the tensions in both the slack and tension sides of the belt. Fig. 3 illustrates the theory of generation of the centrifugal tension Tc.

The length of the arc US in Fig. 3 is
length of arc $US = r.d\theta$
mass of arc $US = m.r.d\theta$
then, the centrifugal force is

$$Fc = (m.r.d\theta)\frac{V^2}{r} = m.d\theta.V^2 \tag{8}$$

From the force balance in Fig. 3, it can be concluded that:

$$Tc.Sin\left(\frac{d\theta}{2}\right) + Tc.Sin\left(\frac{d\theta}{2}\right) = Fc \tag{9}$$

as $Sin\left(\frac{d\theta}{2}\right)$ is small. Therefore, it can be written as $\frac{d\theta}{2}$

$$2Tc\left(\frac{d\theta}{2}\right) = m.d\theta.V^2 \tag{10}$$

Then, the centrifugal tension is:

$$Tc = m.V^2 \tag{11}$$

By calculating the tensions of both the tension side and the slack side and considering the centrifugal tension, the pressure acting on the side of the pulley can be calculated by:

$$P_{pulley} = \frac{[(T_1 + Tc) + (T_2 + Tc)]}{\frac{1}{2}2\pi.r.b} \tag{12}$$

Equation (12) shows the applied pressure at the pulley's half circumference where the belt will be acting.

The pressure P_{pulley} was found to be 0.086 MPa, 0.194 MPa and 0.345 MPa and the corresponding pulley rotations are 2000 rpm, 3000 rpm and 4000 rpm respectively. These pressure values would be used in applying the cyclic loading in the next sections.

4. Finite element modeling

Three finite element models of the pulley were built with four, six and eight bolt holes. ANSYS finite element software was used to build the models. The element types were SOLID186 and SURF154. The element SOLID186 comprised nodes at the element corner and at the mid-point of the element sides,

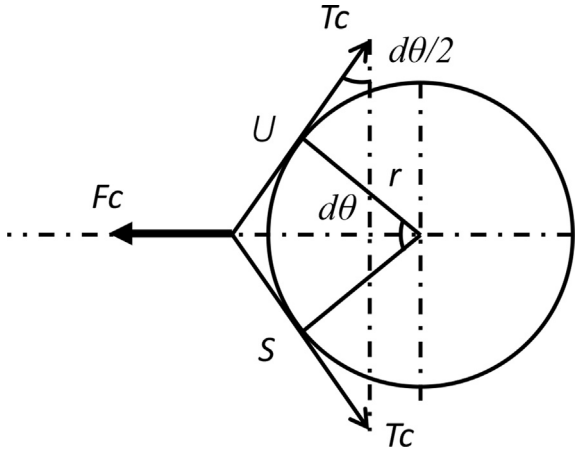

Fig. 3. Generation of centrifugal tension in the belt.

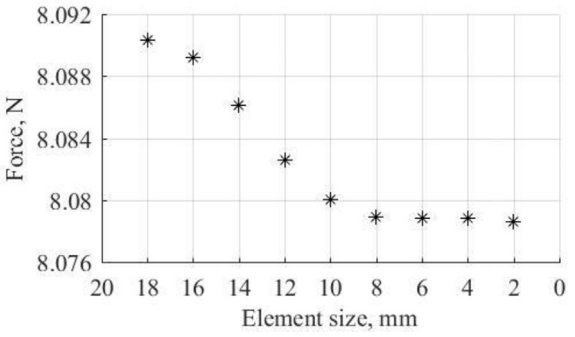

Fig. 4. The element size convergence study.

making a total of 20 nodes per element. The element SURF154 provides the ability to apply loads at the surfaces and has four to eight nodes. The material is steel with Young's modulus of elasticity of 210 GPa and Poisson's ratio of 0.3.

A convergence study was conducted to decide the element size. The convergence curve is shown in Fig. 4. Based on the convergence study, the element size used is 8 mm.

The node number, element number, mass and volume of the three models are shown in Table 2. Fig. 5 shows the three finite element models of pulley with 4, 6 and 8 bolt holes.

5. Stiffness estimation study

Estimation of the stiffness of the pulleys was essential in order to find approximate values for the natural frequency of the pulley models. These values of the natural frequency could then be compared with the natural frequency values obtained from the dynamic analysis (modal analysis) in Section 7.

Estimation of the stiffness of the pulley was conducted through applying ramp displacements of 0.1 mm and 1 mm over 1.5 s and at 10 sub-steps. The displacement was applied at the side of the pulley and the reaction force was measured at the same position. Then the resulted reaction force on the pulley was recorded. Plots of force-displacement were obtained by using the data of the applied displacements and resulted reaction forces. Fig. 6 shows the force-displacement curve for one of the cases.

The stiffness of the model was represented through the slope of the force-displacement curve in each case. The stiffness values for the pulley models with four, six and eight holes were 79.6×10^8 N/m, 95.2×10^8 N/m and 105.4×10^8 N/m respectively.

6. Quasi-static analysis

Quasi-static loading means that the rate of change of the applied load with time is not fast enough to affect the inertia terms of the system [12]. Therefore, a quasi-static cyclic pressure was chosen to apply to the pulley models.

A cyclic pressure was applied to the side of the pulley at the position where the contact was achieved between the belt and the pulley. The cyclic pressure signal was produced by MatLab program. The amplitudes of the signal were 0.086 MPa, 0.194 MPa and 0.345 MPa (Section 3) at a frequency of 1 Hz. The pressure signal had 151 steps over a time of 1.5 s. The pressure was applied to the pulley in a lateral direction.

Pre-pressures of 0.043 MPa, 0.097 MPa and 0.172 MPa were introduced to the signals of 0.086 MPa, 0.194 MPa and 0.345 MPa respectively to ensure compressive loading condition was achieved during the loading cycle. The pressure signal of cyclic loading is shown in Fig. 7. The boundary conditions were applied by fixing (zero displacement in all directions) bolt holes and the shaft hole. The load was applied on half of the outer surface of the pulley.

The resulted deformations and Von-Mises stresses were recorded at 300 steps to ensure high quality resolution for the obtained results signal. The maximum values of the obtained Deformations and stresses are listed in Tables 3 and 4.

Fig. 8 shows a deformed model of the pulley with 6 bolt holes. The resulted deformation signals due to applied cyclic pressure of 0.086 MPa, 0.194 MPa and 0.345 MPa are depicted in Figs. 9–11 respectively. The obtained stress signals at cyclic pressures of 0.086 MPa, 0.194 MPa and 0.345 MPa are depicted in Figs. 12–14 respectively.

Table 2
Data on the FE models.

	Four hole pulley	Six hole pulley	Eight hole pulley
No. of nodes	9973	10,085	10,166
No. of elements	1621	1633	1635
Volume	3.9209×10^5 mm^3	3.9052×10^5 mm^3	3.8895×10^5 mm^3
Mass	3.0779 kg	3.0656 kg	3.0533 kg

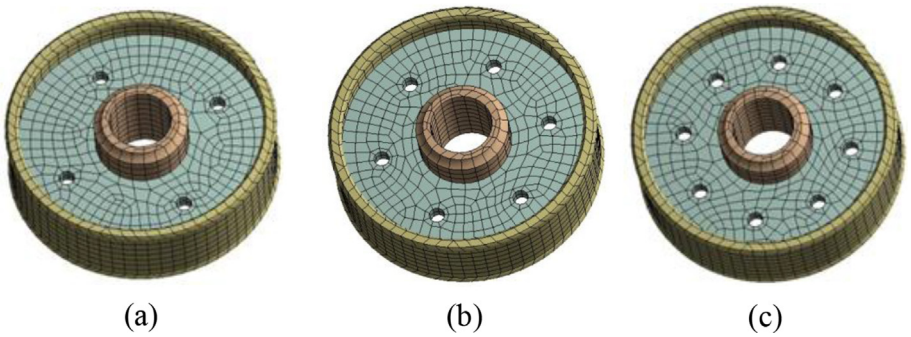

Fig. 5. Finite element models of the pulley with (a) 4 bolt holes, (b) 6 bolt holes and (c) 8 bolt holes.

7. Dynamic analysis

This section investigates the modal response and the frequency response function of the pulley system.

7.1. Modal analysis

Modal analysis is a test performed in the frequency domain. It shows the dynamic characteristics of a system through finding the values of the natural frequency and by describing the mode shapes of a system at each natural frequency. For simple systems such as a simply supported beam or cantilever beam, mode shapes can be plotted through computing and coding mathematical equations. However, for more complex structures, it would be difficult and time consuming to predict the mode shapes [13]. Therefore, these mode shapes were obtained through ANSYS software.

Modal analysis was performed on the three models of the pulley with four, six and eight bolt holes. The boundary condition for this analysis was applying zero displacement in the bolt holes and in the shaft hole.

For each pulley model, the mode shapes and the natural frequencies were recorded and plotted. Table 5 gives the first three natural frequencies for each model.

Through examining Table 5 and Figs. 15 and 16, it can be seen that the different modes share approximately the same natural frequency. This behavior is normal in three dimensional systems as there will be flexural modes and lateral modes in different directions at the same natural frequency value.

For instance, the 1st mode and the 2nd mode of the pulley with 6 bolt holes shown in Fig. 15 are flexural mode shapes but at different directions and this is the reason for them having approximately the same natural frequency value. The same applies for the 3rd and 4th modes depicted in Fig. 16, where the lateral mode shape at different directions is presented. The first four mode shapes for the pulley with six bolt holes are shown in Figs. 15 and 16.

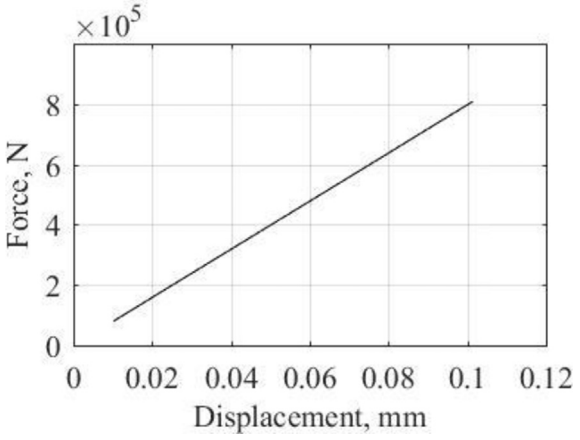

Fig. 6. Force-displacement curve for pulley with 4 bolt holes and loaded with ramp displacement of 0.1 mm.

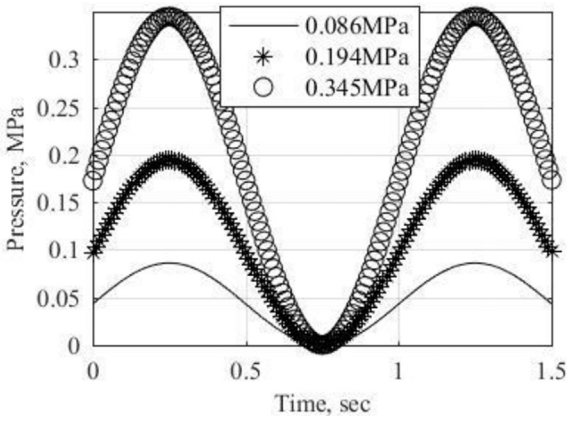

Fig. 7. Cyclic pressure loading signals.

Table 3
Results of maximum deformations in the pulley models during the different cyclic pressure loadings.

Applied pressure, MPa	Deformation, mm		
	Pulley with 4 holes	Pulley with 6 holes	Pulley with 8 holes
0.086	0.49×10^{-3}	0.46×10^{-3}	0.44×10^{-3}
0.194	1.10×10^{-3}	1.10×10^{-3}	1.00×10^{-3}
0.345	2.00×10^{-3}	1.90×10^{-3}	1.80×10^{-3}

Table 4
Results of maximum Von Mises stresses in the pulley models during the different cyclic pressure loadings.

Applied pressure, MPa	Von Mises stress, MPa		
	Pulley with 4 holes	Pulley with 6 holes	Pulley with 8 holes
0.086	2.22	1.88	1.86
0.194	5.09	4.31	4.26
0.345	8.92	7.55	7.46

7.2. Frequency response function (FRF) of the pulley system

Frequency response function is used in this research to measure the response of the different models of the pulley system to excitations of compressive pressure of 0.086 MPa, 0.194 MPa and 0.345 MPa. The FRF is presented in the frequency domain. The range of frequency chosen for the response is 0 Hz–50,000 Hz. The frequency of the data acquisition (resolution) is 10 Hz. The boundary conditions for this analysis require that the surfaces of the shaft and the bolt holes are fixed in all directions and pressures of 0.086 MPa, 0.194 MPa and 0.345 MPa are applied at the half of the pulley that is in contact with the belt. The obtained FRFs for the three models of the pulley: 4 holes, 6 holes and 8 holes, are depicted in Figs. 17–19 respectively.

8. Results and discussion

In this study, models of pulley comprising four, six and eight bolt holes are exposed to cyclic loading. Pulley models are analyzed quasi-statically and dynamically. This section discusses the obtained results in more detail and extracts some conclusions.

For the same pulley model, when increasing the cyclic pressure from 0.086 MPa to 0.345 MPa, the deformations also increased correspondingly as listed in Table 3. This behavior was replicated in all three pulley models (4, 6 and 8 holes). The obtained Von Mises stresses increased with increasing the cyclic

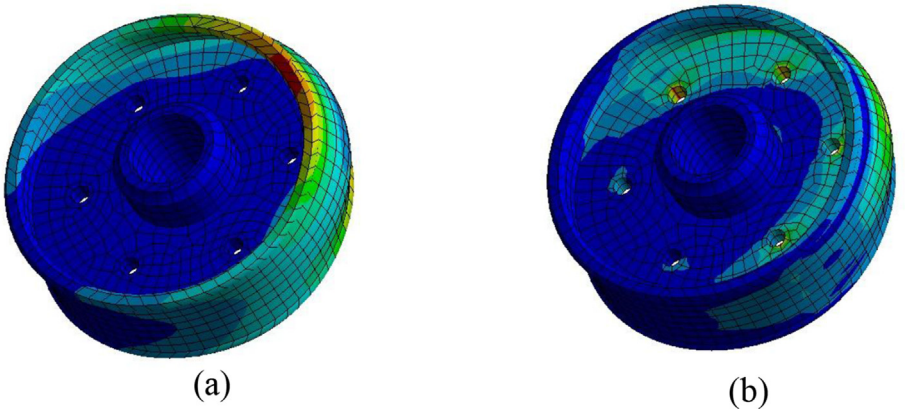

Fig. 8. (a) The deformation and (b) Von-Mises stress for the pulley model with 6 bolt holes and at cyclic pressure of 0.194 MPa.

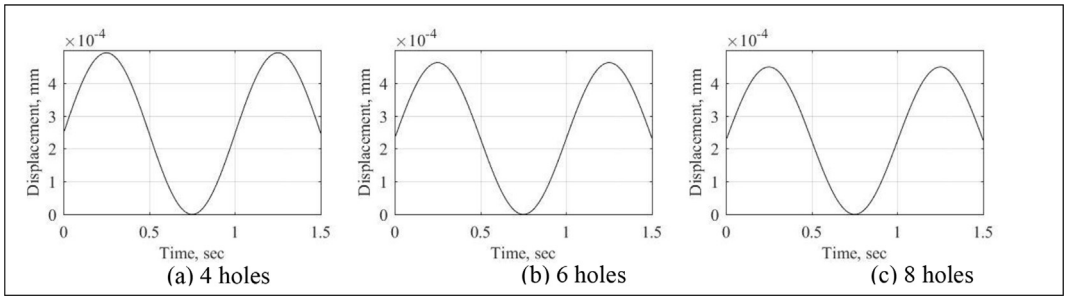

Fig. 9. Results of displacements at cyclic pressure of 0.086 MPa for pulley model.

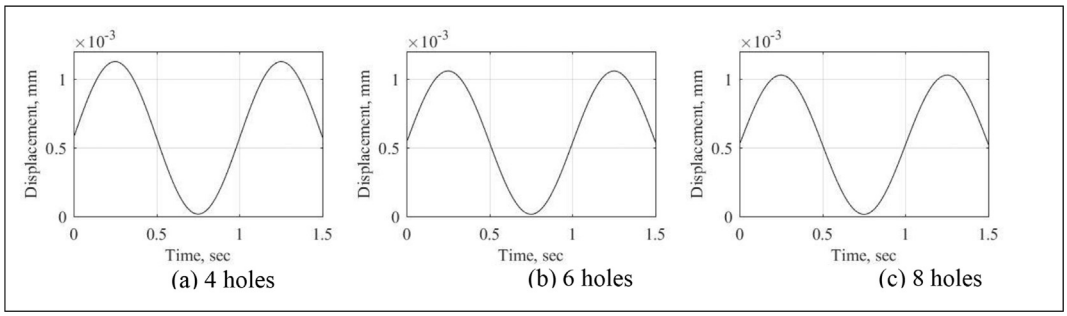

Fig. 10. Results of displacements at cyclic pressure of 0.194 MPa for pulley.

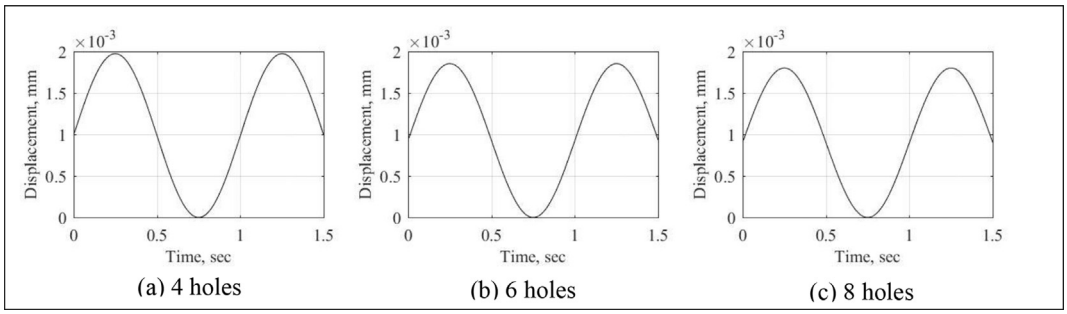

Fig. 11. Results of displacements at cyclic pressure of 0.345 MPa for pulley.

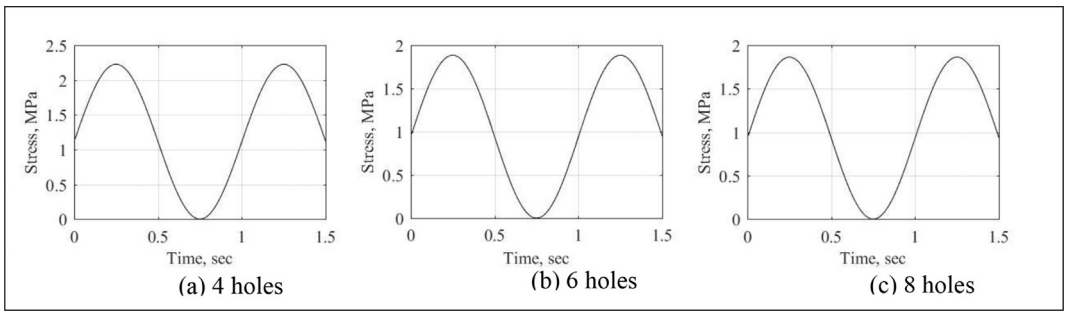

Fig. 12. Results of Von Mises stress at cyclic pressure of 0.086 MPa for pulley model.

pressure from 0.086 Mpa to 0.345 Mpa for the same pulley model, as shown in Table 4. All three pulley models showed similar behavior. For the same pulley model, the above results can simply be attributed to simple mechanics whereby increasing the pressure can increase the resulted deformations and stresses.

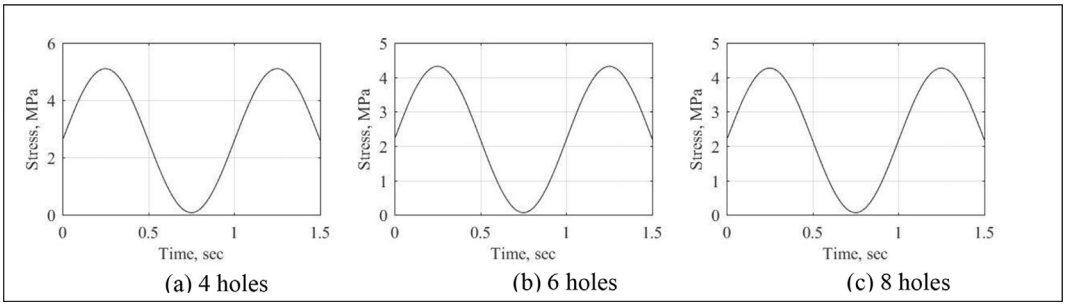

Fig. 13. Results of Von Mises stress at cyclic pressure of 0.194 MPa for pulley model.

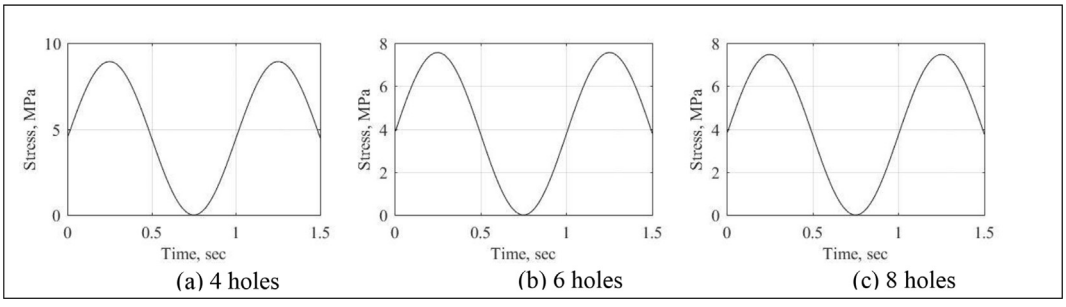

Fig. 14. Results of Von Mises stress at cyclic pressure of 0.345 MPa for pulley model.

Table 5
Natural frequencies of the 4 holes, 6 holes and 8 holes pulley models.

Mode	Natural frequency, Hz		
	Pulley with 4 holes	Pulley with 6 holes	Pulley with 8 holes
1	9940	10,550	10,800
2	15,660	16,610	16,930
3	23,440	26,890	30,280

In this research, pulley models with 4, 6 and 8 bolt holes were used to investigate the effect of increasing the number of holes on the dynamic characteristics of the pulley system. Increasing the number of holes in the pulley model increased the stiffness of the pulley system. The stiffness was 79.6×10^8 N/m, 95.2×10^8 N/m and 105.4×10^8 N/m for pulleys with 4, 6 and 8 holes respectively. Of course, the mass was decreased by increasing the number of holes in the pulley model. The mass was 3.0779 kg, 3.0656 kg and 3.0533 kg for pulleys with 4, 6 and 8 holes respectively. The results for stiffness and mass will have an effect on the natural frequency of each pulley model depending on the number of holes.

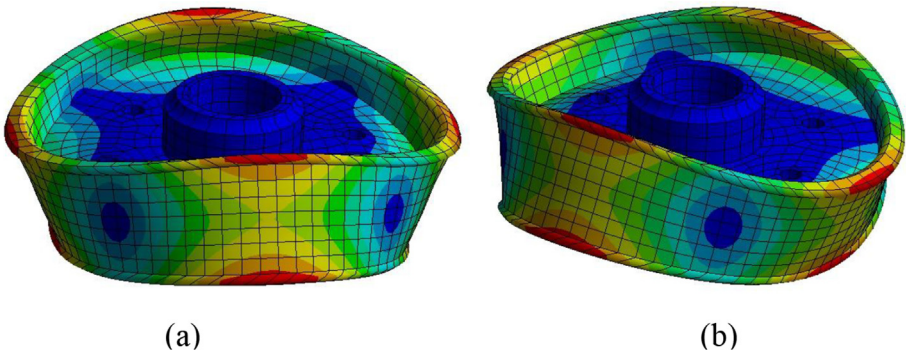

Fig. 15. (a) First and (b) second flexural mode shapes of the pulley with 6 bolt holes.

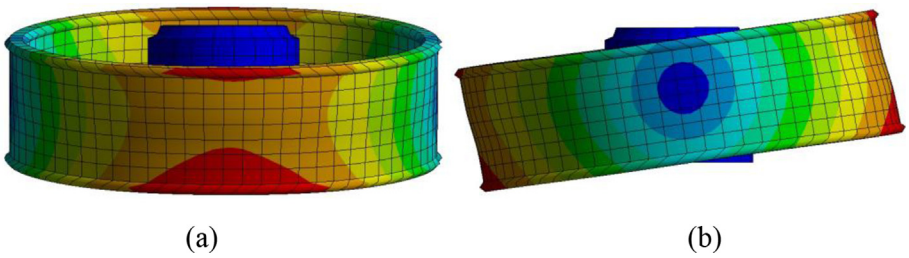

Fig. 16. (a) Third and (b) fourth lateral mode shapes of the pulley with 6 bolt holes.

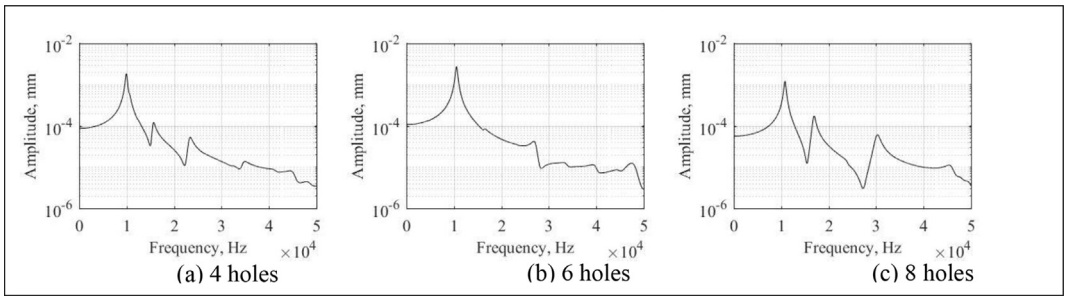

Fig. 17. Frequency response functions at cyclic pressure of 0.086 MPa for pulley model.

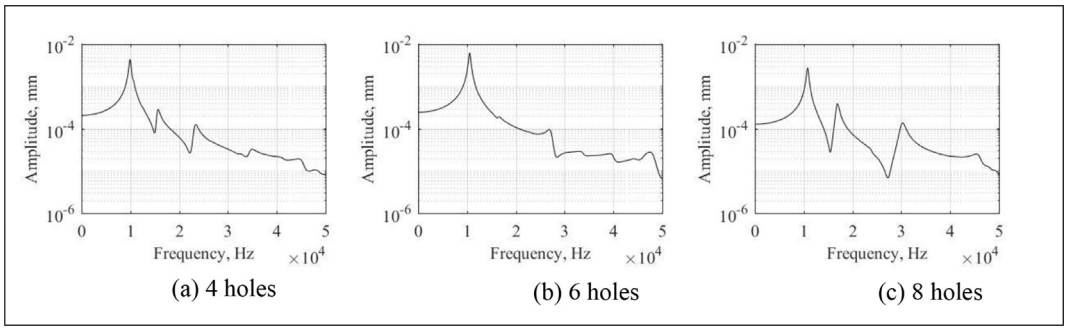

Fig. 18. Frequency response functions at cyclic pressure of 0.194 MPa for pulley model.

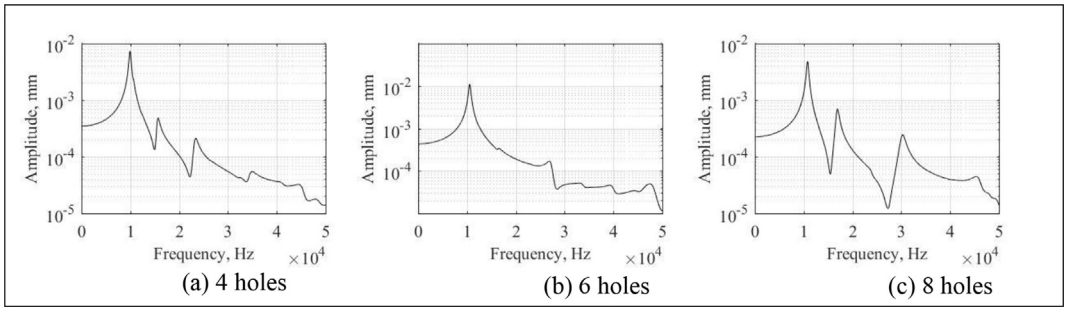

Fig. 19. Frequency response functions at cyclic pressure of 0.345 MPa for pulley model.

Increasing the number of holes in the pulley decreased the resulted deformations and stresses for the same applied cyclic pressure, as shown in Tables 3 and 4 This was due to the increased stiffness caused by increasing the number of holes as discussed in the above paragraph.

The natural frequency of the pulley was increased by increasing the number of holes in the pulley model, as shown in FRF plots (Figs. 15−17) and as listed in Table 5. Increasing the cyclic pressure had approximately no effect on the natural frequency.

9. Conclusions

In this paper, pulley designs with four, six and eight bolt holes were dynamically investigated. The study concluded that higher stiffness and higher natural frequency values were obtained with eight bolt holes than when using four bolt holes. Also, the resulted deformations and stresses reduced due to the increase in stiffness obtained with eight bolt holes. For the same pulley model, increasing the cyclic loading has increased the resulted deformations and stresses.

Based on the obtained results, more effective and stiffer pulley can be obtained by using eight bolt holes than using four bolt holes. This fact increases the working abilities of the pulley at higher ranges of engine run.

References

[1] R. Uddanwadiker, Effect of rim thickness on load sharing in the rotating elements, Am. J. Mech. Eng. 1 (2013) 126−130, https://doi.org/10.12691/ajme-1-5-4.

[2] K.S.R.R. Veenitha Yalavarthi, Ramu Kandregula, Experimental analysis of stress, strain and deformation on different types of conveyor belt pulleys. An analysis conducted at Visakhapatnam Steel Plant, Aust. J. Basic Appl. Sci. 10 (2016) 715−719.

[3] D. Singathia, M.L. Aggarwal, Finite element modeling for replacement of C . I . pulley with suitable material, Int. J. Mod. Eng. Res. 2 (2012) 3028−3031.

[4] M. Madhavi, R.J. Kumar, P. Padmavathi, Modeling and analysis of a pump pulley, Int. J. Adv. Res. Sci. Eng. 7 (2018) 561−570.

[5] B. Kim, Y. Kim, D. Chun, S. Ahn, J. Jang, Durability of automotive V-belt pulley, Int. J. Automot. Technol. 10 (2009) 73−77.

[6] J. Mo, Y. Yuan, Finite element analysis and calculation of HTC15J01 petrochemical industry crane pulley design, Chem. Eng. Trans. 71 (2018) 1045−1050, https://doi.org/10.3303/CET1871175.

[7] C.A. Rinaldini, E. Mattarelli, T. Savioli, G. Cantore, M. Garbero, A. Bologna, Performance, emission and combustion characteristics of a IDI engine running on waste plastic oil, Fuel 183 (2016) 292−303, https://doi.org/10.1016/j.fuel.2016.06.015.

[8] İsmet Sezer, Thermodynamic, performance and emission investigation of a diesel engine running on dimethyl ether and diethyl ether, Int. J. Therm. Sci. 50 (2011) 1594−1603.

[9] K. R, in: Theory of Machines, fourteenth ed., S. Chand & Co., New Delhi, 2005.

[10] Density of Rubber, manufactured (material). https://www.aqua-calc.com/page/density-table/substance/rubber-coma-and-blank-manufactured, 2019. (Accessed 5 December 2019).

[11] H. Asker, J. Rongong, C. Lord, Mathematical and numerical evaluation of the damping behaviour for a multi-strand bar, 6th, Eur. Conf. Struct. Control. 6 (2016) (2016) 1−10.

[12] H. Asker, J. Rongong, C. Lord, Stiffness and loss factor of unbonded, multi-strand beams under flexural deformation, Int. Conf. Eng. Vib. 11 (2015) (2015) 1518−1529.

[13] H. Asker, J. Rongong, C. Lord, Dynamic properties of unbonded, multi-strand beams subjected to flexural loading, Mech. Syst. Signal Process. 101 (2018) 168−181.